PAPER

Check for updates

Chitosan-*g*-oligo/polylactide copolymer non-woven fibrous mats containing protein: from solid-state synthesis to electrospinning

Tatiana S. Demina, [ID] *[ab] Anastasia S. Kuryanova,[bc] Nadejda A. Aksenova,[bc] Andrey G. Shubnyy,[d] Tatiana N. Popyrina,[a] Yaroslav V. Sokovikov,[e] Elena V. Istranova,[b] Pavel L. Ivanov,[a] Peter S. Timashev [ID] [bcd] and Tatiana A. Akopova [ID] [a]

Graft-copolymers based on bioresorbable synthetic (oligo-/polylactide) and natural (chitosan and collagen/gelatin) components were synthesized through solid-state reactive co-extrusion and used for fabrication of fibrous non-woven mats *via* the electrospinning technique. The effect of the macromolecular features of the initial components on the copolymer characteristics was evaluated using FTIR-spectroscopy, differential scanning calorimetry and elemental analysis. Dynamic light scattering analysis showed that the copolymers have a tendency to form stable ultra-fine dispersions with a mean size of macromolecular aggregates of 150 nm within chlorinated solvents. The copolymer-containing non-woven fibrous mats were fabricated *via* an electrospinning procedure using chloroform as a solvent. An effect of the copolymer composition on the casting solution's viscosity, conductivity and surface tension was evaluated. Scanning electron microscopy showed that the obtained mats consist of randomly distributed fibers with a mean size of ~5 μm and a more complex morphology than mats fabricated from neat polylactide. The proposed mechanochemical approach to obtain hybrid copolymeric compositions differs from typical liquid-phase methods in terms of high efficiency, simplicity and cleanness.

Introduction

Various biocompatible scaffolds for tissue engineering based on synthetic and natural polymers are proposed to provide enhanced cell adhesion and proliferation on their surfaces. Since these scaffolds act as temporary templates to support cell growth, they should have an optimum structure (*e.g.* surface topography and chemistry, porosity, pore interconnectivity, *etc.*), to provide efficient cell delivery; to possess desirable mechanical properties as supports for cell growth; to be biocompatible and bioresorbable with the same rate as the new tissue formed.[1,2] One of the promising pathways to create new biocomposite materials for the regeneration of damaged tissues is the production of micro/nano-fibrous scaffolds. Such materials are characterized by an extraordinary large surface area per unit mass, and low basis weight of the material for implantation with high permeability.[3–5] Another advantage is the ability to control the orientation of cell growth, which is determined by the orientation of the fibers in the scaffold.[6,7] It should also be noted that the diameter of the fibres and fibrils of some tissues and the extracellular matrix is approximately the same; therefore, the fibres are simulated and can replace the latter one.[8,9]

In terms of mechanical properties and processability, synthetic polyesters, *i.e.* polylactide, polyglycolide, poly-caprolacton, and their copolymers are particularly attractive.[10–13] However, a lack of functional groups promoting cell attachment limits their usage in bioengineering. Besides, polyesters show undesirable host reactions such as inflammatory and allergenic reactions due to a decrease of local pH as a consequence of their hydrolytic degradation.[14,15] Natural polymers have a diverse set of functions in their native setting, and are widely used for pharmaceutical and medical applications mostly due to their biodegradability and good cell adhesion.[16–19] For example, collagen and gelatin are important components in tissue and organ development and regeneration. They possess an ability to form complexes with polyions that makes these polymers attractive for drug delivery and tissue engineering applications.[20] Another natural polymer of cationic origin, chitosan, is a linear polysaccharide consisting of β(1→4) linked D-glucosamine residues with a variable number of randomly located *N*-acetyl-glucosamine groups. The electrostatic interactions with negatively charged biomolecules are of great interest because allow

[a]Enikolopov Institute of Synthetic Polymeric Materials, Russian Academy of Sciences, 70 Profsoyuznaya St., Moscow 117393, Russia. E-mail: detans@gmail.com

[b]Institute for Regenerative Medicine, Sechenov University, 8-2 Trubetskaya St., Moscow 119991, Russia

[c]Semenov Institute of Chemical Physics, Russian Academy of Sciences, 4 Kosygina St., Moscow 119991, Russia

[d]Institute on Photon Technologies, Federal Scientific Research Centre "Crystallography and Photonics", Russian Academy of Sciences, 2 Pionerskaya St., Troitsk, Moscow 142190, Russia

[e]Scheltec AG, 19 Kosygina Str., Moscow, 119334, Russia

retain and concentrate growth factors secreted by colonizing cells. Moreover, the N-acetyl-glucosamine moiety in chitosan holds the specific interactions with growth factors, receptors and adhesion proteins.[21–23] Some researchers reported that chitosan enhanced functions of inflammatory cells, namely polymorphonuclear leukocytes, macrophages and fibroblasts promoting granulation and tissue organization.[24,25]

Thus, the choice of suitable material for the scaffold preparation plays a crucial role for the success of the application. Composite systems which combine properties of synthetic and natural polymers, in particular polysaccharides and polylactide attract attention of many researchers as a perspective approach to prepare an "ideal" scaffold.[26–28] Various neat biocompatible polymers (polysaccharides, proteins, polymers and copolymers of lactide) as well as their derivatives and mixtures were used to produce fibrous materials via electrospinning technique.[29–33] In order to form micro/nano-sized fibres, hybrid polymeric materials should be capable of dispersing at least at a colloidal level in suitable solvents. Toxic solvents such as trifluoroacetic acid should be used to obtain chitosan/PLA blend homogeneous solutions.[34] Grafting and cross-coupling reactions of polymers may contribute to this behaviour. Of course, there are many processing obstacles typical for chemical interaction of polymers of very different origins when it proceeds under traditional liquid-phase conditions, i.e. the difficulty of selecting a joint solvent, the need to use toxic catalysts and low productivity due to the low concentration of reactants. Mechanochemistry, which relays upon an activation of solid substances and intensive intermixing by applying shear deformation, could be a more effective and successful approach to copolymer synthesis.[35,36]

In this study, we developed mechanochemical synthesis of graft copolymers consist of bioresorbable synthetic (oligo-/polylactide) and natural (chitosan and collagen/gelatin) components. An effect of the copolymer compositions on dispersability in chlorinated solvents and their processability via electrospinning procedure was evaluated. Techniques such as Fourier Transform Infrared Spectroscopy (FTIR), Dynamic Light Scattering (DLS), Differential Scanning Calorimetry (DSC), Scanning Electron Microscopy (SEM) and elemental analysis were used for characterization.

Experimental

Materials

Commercially available poly(L-lactide) (PLLA) ("Sigma-Aldrich", Germany) with an average M_w of 160 kDa; chitosan type I with M_w = 350 kDa and acetylation degree (DA) of 0.14 ("Sonat", Russia); gelatine ("Chimmed", Russia) were used throughout this study as received. Chitosan type II (M_w = 60 kDa; DA of 0.10) was prepared by the solid-state synthesis in ISPM RAS as reported earlier.[37] Oligo(L-lactide) of M_w of 5 kDa was synthetized from L-lactic acids (Panreac, Spain) using 0.001% $SnCl_2$ as catalyst. Collagen (type I) was obtained from cattle dermis as reported earlier.[38,39] All solvents were purchased from Acros Organics (Belgium) as analytical grade and were used without further purification.

Copolymer synthesis and characterization

Chitosan-g-oligo/poly(L-lactide) copolymers contained collagen or gelatine were synthesized under shear deformation in a pilot co-rotating twin-screw extruder (ZE40×23D, Berstorff, Germany) specially designed for powerful dispersion of solids.[40–43] The chitosan (type I)/oligo(L-lactide)/collagen and chitosan (type II)/poly(L-lactide)/gelatine copolymers were prepared at component weight ratios of 46.5/50/3.5 and 35/52/13 and marked as CO-C and CP-G, respectively. The co-extrusion temperature was below melting point of the synthetic component and was 55 °C and 100 °C for CO-C and CP-G, respectively.

Fractionation of the prepared copolymers in chlorinated solvents was performed as followed: the sample probe (~1 g) was dissolved in 50 mL of CH_2Cl_2 under magnetic stirrer agitation for 2 hours at RT; the stable colloidal fraction was carefully selected after solution kept idle within 48 h. The cycle of selections was repeated several times with new portion of organic solvent until optically transparency of the solution. The stable fractions selected during all cycles as well as the part of the copolymer remained in the tube were dried in vacuum oven and measured.

For the acidic medium fractionation, a portion of ~1 g taken from the sample was immersed into 75 mL of 2% acetic acid. After stirring for about 24 hours at RT, insoluble fractions were collected by filtration, washed on the filter with distilled water to reach neutral pH and freeze-dried. The solids contained in the filtrate were precipitated by adding an equal amount of 5% ammonia aqueous solution, separated from the solutions by centrifugation, washed with water to reach neutral pH and freeze-dried.

Solubility characteristics of the copolymer dispersions in CH_2Cl_2 (0.2 mg mL^{-1}) were assessed by DLS using a Zetatrac particle size analyser (Microtrac, Inc., USA) and Microtrac application software program (V.10.5.3).

CHN elemental composition of the stable in methylene chloride fractions of the copolymers was carried out using a FLASH-2000 Organic Elemental Analyzer (Thermo, UK). The percentage of carbon, hydrogen and nitrogen was estimated.

FTIR analysis of the initial components and the synthesized graft-copolymers was carried out using Spectrum Two FT-IR Spectrometer (PerkinElmer, USA) in ATR mode. The spectrometer feature: high-performance, room-temperature LiTaO₃ MIR detector, standard optical system with KBr windows for data collection over a spectral range of 8300–350 cm^{-1} at a resolution of 0.5 cm^{-1}. All spectra were initially collected in ATR mode and converted into IR-transmittance mode. Spectra of non-modified chitosan and its copolymers were normalized using an intensity of C–O stretching vibrations of pyranose cycle band (1081 cm^{-1}) as internal standard.

DSC measurements were performed using a STA 6000 simultaneous thermal analyser (PerkinElmer, USA). Samples for DSC experiments (about 10 mg) were encapsulated in standard PerkinElmer aluminium pans and heated in a nitrogen medium at a gas flow rate of 40 mL min^{-1} and linear heating rate of 20 °C min^{-1}. Process was described via temperature dependence of thermal effects with measuring errors of ±1.5 °C and ±2%, respectively.

Fabrication and characterization of non-woven mats

The fibrous electrospun non-woven scaffolds were fabricated from 10 wt% solutions of neat PLLA or its mixtures with CO-C and CP-G at 9.5/0.5 w/w ratio in chloroform using nozzle technology.

Viscosity (η) of the prepared solutions was measured using electromagnetically spinning viscometer EMS-1000 (Kyoto Electronics Manufacturing, Japan). All measurements were carried out at 25 °C, after a rest time of 3–5 min, applying a shear rate of 400 s^{-1}.

Electrical conductivity was evaluated with an aim of Expert-002 conductometer (Volta, Russia). Surface tension (σ) was calculated from contact angles (θ) acquired using Acam-MSC01 (Apex Instruments, India). The eqn (1) used for the calculation was as followed:

$$\sigma = d^2 pg/H \tag{1}$$

where d – diameter of the drop, p – density of the solution ($p = m/v$, where m – weight of solutions, v – volume of the solutions), g – gravitational acceleration, $1/H = d/2h$, where h – height of the drop.

For electrospinning, the laboratory-made set-up equipped with a high-voltage power supply (VIDN-30, "OST", Russia) was used. The prepared solutions were loaded in a plastic syringe with G22 needle of 0.7 mm. The applied voltage was 25–30 kV, the flow rate was set at 0.1–0.2 mL h^{-1} and the distance between the needle tip and the cupper plate support (10 × 7.5 mm) as a conductive static collector was 21–25 cm. A preliminary optimization of the electrospinning conditions in terms of solvent nature, PLLA concentration and a needle type was carried out.

The morphology of the fabricated electrospun scaffolds was studied by SEM using Phenom ProX (PhenomWorld, Netherlands) at 10–15 kV. To calculate an average fiber diameter and its distribution, the SEM images were analysed using ImageJ software (version 1.52). At least 700–800 fibres were taken at random to carry out this estimation. Presence of natural components onto the fibrous mat's surface was detected using fluorescein isothiocyanate (FITC) (Sigma-Aldrich) as selective label according to the procedure described previously.[44] Briefly, sample pieces (5 × 5 mm) were incubated in 500 μL of borate buffer (pH 8.3), then, 50 μL of FITC (0.2% in dimethyl sulfoxide) were added. After keeping the samples in dark place for 24 h they were carefully washed with water and observed with a microscope Leica DFC7000T (Leica Microsystems, Germany).

Results and discussion

Characterization of the prepared copolymers

Amphiphilic nature of both copolymers should affect their affinity to various solvents. Generally, these copolymers are differing in length of hydrophilic and hydrophobic fragments: CO-C contains collagen and chitosan of high M_w (350 kDa) with grafted oligolactide (M_w 5 kDa) moieties, while CP-G is based on polylactide with high M_w (160 kDa), but rather low-molecular-weight hydrophilic components, *i.e.* gelatin and chitosan with M_w of 60 kDa. Solubility data of the copolymers are summarized in Table 1. Neat chitosan and proteins were easily dissolved in 2% acetic acid. The grafting of hydrophobic oligo/polylactide moieties led to their partial insolubility in medium and dispersability in organic chlorinated solvent which is extraneous for non-modified polysaccharides and proteins.

Each of the soluble/insoluble fractions in both solvents characterizes a part of macromolecules enriched with either hydrophobic oligo/polylactide fragments or hydrophilic natural polymers. As could be seen in Table 1, the CP-G copolymer prepared with high-molecular-weight polylactide as a hydrophobic component and low-molecular-weight natural polymers demonstrates a better affinity to CH_2Cl_2 than oligolactide-contained copolymer. On the other hand, natural components with a higher molecular weight provide enhanced solubility of the amphiphilic copolymers in aqueous media.

It should be specially noted that the both copolymers are not giving true solutions neither of those solvents and a totally differ in solubility behaviour from physical mixture of components. Since an ability of the copolymers to form fine dispersions within chlorinated solvents is a more interesting in terms of practical application as a part of this work, the dispersions in methylene chloride were analysed in a more details. Although the keeping rest of the solutions led to a gradual formation of large associates, which precipitate in CH_2Cl_2, a part of hydrophilic moieties was stabilized within organic solution according to elemental analysis data. So, the stable in CH_2Cl_2 fractions of CP-G copolymer contained 0.75 ± 0.06 wt% of nitrogen, thus indicating that up to 8 wt% of nitrogen-containing components (chitosan and gelatine) were bounded with the polylactide.

DLS data show bimodal distribution for both CO-C and CP-G copolymers in methylene chloride. As could be seen in Fig. 1 they formed a large number (~90%) of aggregates with a mean size of ~150 nm and a small part of the particles with submicron distribution level. Interestingly, the CO-C sample containing longer fragments of natural polymers showed the smaller size of the associates and their more uniform distribution than ones of CP-G. That, as well as the bimodal function of size distribution could be caused by different mechanism (intra- or intermolecular interaction) and kinetics of macromolecule associate's formation.

Taking into account functionality of all initial components, there are several reaction routes of grafting.[43] An aminolysis of

Table 1 Fractional analysis of the copolymers in various solvents

Sample	Aqueous solvent (2% CH$_3$COOH)		Chlorinated solvent (CH$_2$Cl$_2$)	
	Soluble fraction, wt%	Insoluble fraction, wt%	Soluble fraction, wt%	Insoluble fraction, wt%
CO-C	63.3	36.7	26.4	73.6
CP-G	53.0	47.0	33.0	67.0

Fig. 1 Size distribution of the 0.2 wt% copolymer dispersions in CH_2Cl_2.

Fig. 3 FTIR spectra initial components, CO-C and CP-G samples.

polylactide ester bonds by amine groups of the natural polymers should be the preferable channels due to their relatively large nucleophilicity as compared with the hydroxyl groups (Fig. 2). Terminal carboxyl groups of oligolactide could be involved in amidation reaction as well. Statistical nature of all these reactions predetermines a wide distribution of macromolecules in terms of their chemical structure, such as a number and length of grafted chains. The latter, undoubtedly, also affects the behaviour of the obtained copolymer systems in various solvents.

Since these grafted copolymers form colloidal solutions in both aqueous and organic solvents, a detailed study of the macromolecular structure of the separate fractions using classical analytical methods is rather difficult; FTIR spectroscopy of initial components and the whole copolymer systems was performed (Fig. 3). Spectra of initial components, *i.e.* chitosan, polylactide and gelatine showed all expected characteristic bands. The spectrum of chitosan presents well-resolved bands of bending vibrations of NH$_2$-groups at 1588 cm^{-1} and amide I at 1650 cm^{-1}, which intensities are in a good correlation with DA. The main protein bands of gelatine, namely amide I (1630 cm^{-1}), amide II (1530; 1449 and 1391 cm^{-1}) and amide III (wide band at 600 cm^{-1}) are also well-defined. The FTIR spectrum of neat polylactide contains a prominent peak of the C=O stretching in ester group (1748 cm^{-1}), the asymmetric C–O–C stretching (1181 cm^{-1}) and symmetric CH$_3$ stretching (1083 cm^{-1}). The spectra of the CO-C and CP-G samples show bands coming from all initial components. For example, the bands of C=O groups are well-resolved in both cases with logical lower intensity than in the homopolyester and with minor shift of its position. The main changes were observed in the amine–amide regions (from 1650 to 1530 cm^{-1}). The band of primary amino groups
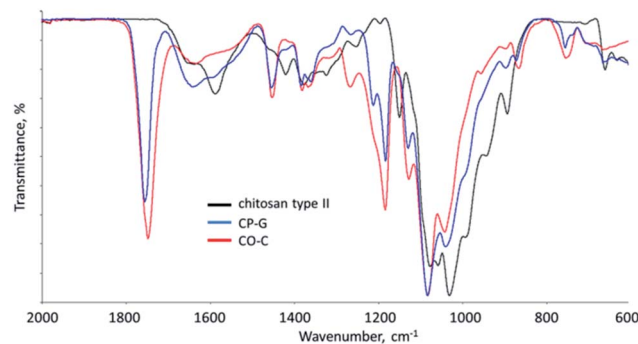
(1588 cm^{-1}), quite intense in comparison with Amide I in the spectrum of the original chitosan, becomes weak in the copolymers spectra, that confirms consumption of amino groups in the reactions. As it was observed in the previous study of chitosan/oligolactide copolymers, this frequency range overlaps also with the carboxylate ion stretching vibrations (about 1580 cm^{-1}) due to partial salt linkages formation.[42]

Fig. 2 Scheme of aminolysis reaction of oligo/polylactide's ester bonds by chitosan amino groups.
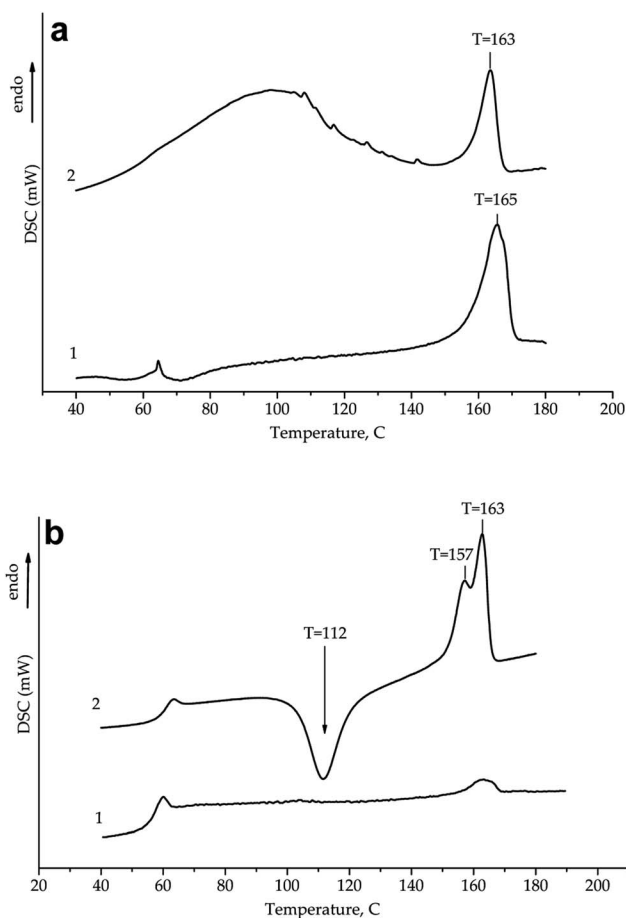

Fig. 4 First (a) and second (b) heating DSC curves for (1) initial PLLA and (2) CP-G. DSC thermograms are offset along the ordinate axis for clarity.
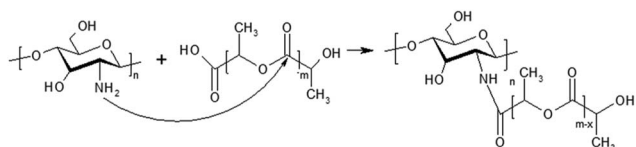
To highlight changes in the polyester part of the copolymers, DSC analysis was carried out. DSC curves obtained on heating the neat PLLA and as-prepared CP-G copolymer are given in Fig. 4a. At first heating run, the PLLA homopolymer demonstrated a glass transition at 61.2 °C and the melting peak at T_m = 165.5 °C with ΔH = 40.6 J g^{-1}. The thermogram of the CP-G copolymer showed an overlapping endotherm at 50–130 °C referred to intensive desorption of water and the melting peak at relatively lower T_m (163 °C) than that for neat PLLA. Neither chitosan nor gelatine revealed sharp endothermic transitions within a temperature range of 130–190 °C, and hence all the endotherms within this range originated from PLLA melting. A presence of chitosan and gelatin led to decreasing of heat of fusion to 20.6 J g^{-1} and complexity of melting endoterms of polyester moieties, and it was more pronounced during the second run (Fig. 4b). An appearance of new complementary peaks indicated specific interaction of polylactide chains with chitosan/gelatine moieties, as described earlier.[43]

Strong exothermic peak observed at the second DSC heating run in the temperature range of 100–130 °C belongs to a cold crystallization of PLLA chains. The fact that we did not observed any crystallization exotherm for PLLA homopolymer at the same conditions inferred that micro-sized chitosan and gelatine exerted clear nucleating effect on the process. This observation is similar to that pointed out previously[45,46] and can lead to faster cycles of processing (e.g. by electrospinning technologies).[26]

Thus, the synthesized graft-copolymers possessed a prominent ability to form ultra-fine dispersions in chlorinated solvents and therefore could be used for formation of polylactide-based materials using electrospinning.

Non-woven mats fabrication and characterization

Here we have studied an effect of copolymer type on the electrospun fibre diameter and morphology of the non-woven scaffolds. Rheological properties and conductivity of the casting solutions are summarized in Table 2. PLLA solution showed higher viscosity values than that containing the copolymers. It can be seen that relatively low molecular weight moieties of natural polymers affect the viscosity of the PLLA solution more significantly than longer ones (cf. viscosity of CP-G and CO-C samples). The same dependence is also characteristic of the values of surface tension of the studied samples. The conductivity of the copolymer-contained casting solutions was

Table 2 Characteristics of the solutions used for electrospinning

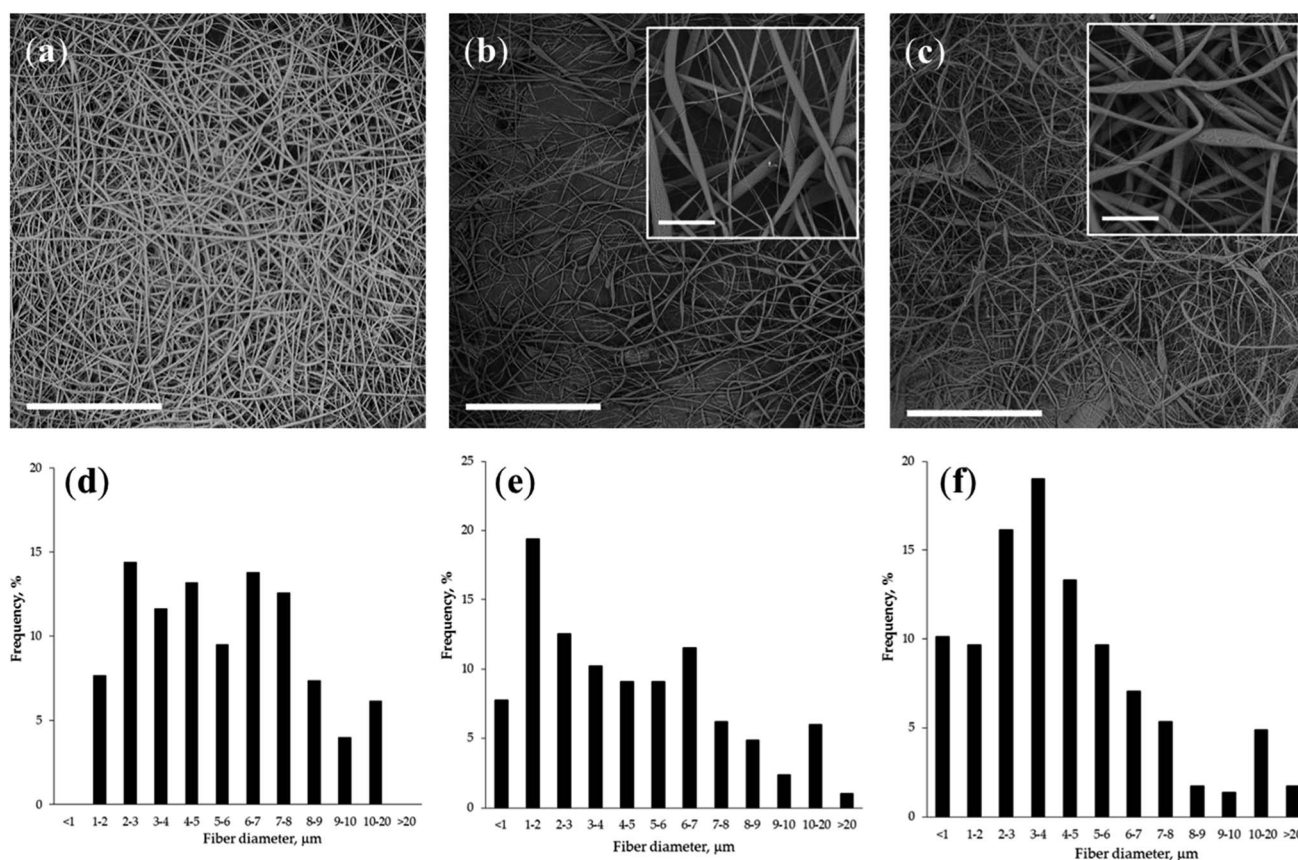| Sample	η, mPa s	Conductivity, µS cm^{-1}	θ, degree	σ, mN m^{-1}
PLLA	607 ± 20	0.010 ± 0.003	28.6 ± 2.5	48.5 ± 4.0
PLLA/CO-C	555 ± 20	0.126 ± 0.005	60.8 ± 3.1	30.0 ± 3.9
PLLA/CP-G	347 ± 20	0.118 ± 0.006	51.9 ± 3.3	23.4 ± 6.1

Fig. 5 SEM micrographs (a, b and c) and histograms (d, e and f) of fibre diameter distribution for non-woven mats fabricated from PLLA (a and d), PLLA/CO-C (b and e) and PLLA/CP-G (c and f). Scale bar is 300 µm for the survey images and 30 µm for the inserted ones.

higher than that of neat PLLA by an order of magnitude. The main functional groups that carry a charge when an electric field is applied and determine the electrokinetic properties of the natural components are: –COOH groups of aspartic and glutamic acid, –NH$_2$ groups of chitosan, lysine, and hydroxylysine, and –NH–C(NH)–NH$_2$ groups of arginine.

At the same time, all the conductivity values were at the lower threshold of those to ensure a stable process of conductivity. However, all polymer compositions have been successfully used for electrospinning to form mats consisting from fibres with a diameter in the range of 1–20 μm. SEM micrographs and fibre diameter distribution for the non-woven mats fabricated from PLLA homopolymer and composite colloidal systems are presented in Fig. 5. The impact of all parameters – viscosity, surface tension and conductivity, on the size of electrospun fibres has not been pronounced. The dispersion state revealed by the DLS had some influence on this indicator. The mean fibre diameter of the PLLA/CO-C and PLLA/CP-G non-woven mats was the similar (4.8 ± 3.9 and 4.6 ± 3.9 μm, respectively), whereas the bulk of the CP-G-based mats lays in the range of 2–4 μm *vs.* 1–3 μm for the CO-C sample. The fibres of PLLA homopolymer also demonstrated wide size distribution with a mean diameter of 5.5 ± 2.7 μm.
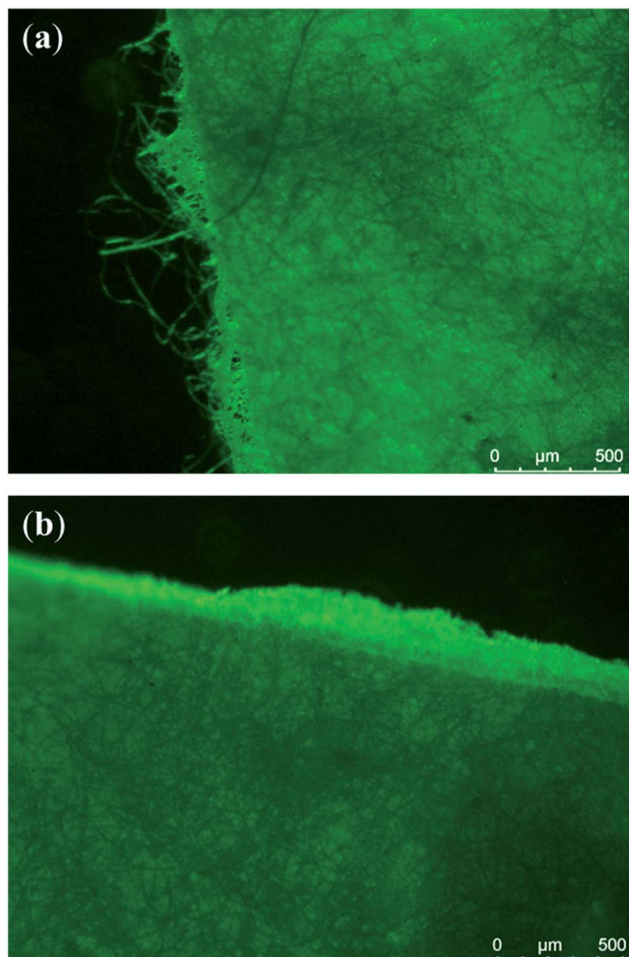
The addition of the polylactide copolymers with chitosan/protein moieties to the neat PLLA solution was found to be very important for the final morphology of microfibers. As could be seen from insets in Fig. 5, presence of copolymers within casting solution yielded fibres with a pronounced surface roughness. The same observation as well as decreased polyester crystallinity was made by Zhu and co-authors at fabrication of electrospun poly(ε-caprolactone)/gelatine scaffolds.[47] Additionally, these fibres have a flatter structure compared to neat polylactide fibres. The complex structure and a rough fibre surface could be an advantage in point of a cell adhesion improvement and wetting behaviour of the non-woven mats, which may serve as efficient scaffolds in tissue engineering.[48–50] Keeping in mind this future application a qualitative analysis of the fibrous mat's surface chemistry was carried out using fluorescein molecule FITC, which is selectively reactive toward chitosan/protein amino groups. As could be seen in Fig. 6 fluorescent microscopy of copolymer-contained mats confirms a presence of natural components onto the surface that are highly desired for enchantment of adhesion and growth of substrate-depended cells.

The presence of protein components in casting solutions also could be an additional benefit for further development of non-woven scaffolds loaded with bioactive components and other additives in their structure, since gelatin particles have been demonstrated to be effective lyophilic stabilizer of lyophobic colloidal systems.[51–53]

Conclusions

In this study, we've prepared and studied the amphiphilic copolymers of chitosan with oligo/polylactide grafted chains additionally contained collagen or gelatin moieties. Low-temperature mechanochemical synthetic approach was used and allowed us to realize an efficient interaction of the components of different hydrophilicity that results in copolymer systems, which are capable of dispersing at a colloidal level in chlorinated solvents. The obtained copolymers were found to be able to increase electrical conductivity of the PLLA solution in chloroform. They were successfully used for fabrication of non-woven mats *via* electrospinning technology. Statistical nature of possible reaction channels determines a wide range of macro-molecular associates formed in the casting solutions that resulted in the complex non-woven microstructure and rough fiber morphology. Combination of bioresorbable synthetic and natural components could be a benefit in terms of further potential of the fabricated non-woven materials for various biomedical applications, especially, in the course of formation of hollow organ tissues, such as urethra, trachea, *etc.*

Conflicts of interest

There are no conflicts to declare.

Acknowledgements

Fig. 6 Fluorescent micrographs of PLLA/CO-C (a) and PLLA/CP-G (b) non-woven mats after their labeling with FITC.

References

1 F. J. O'Brien, Biomaterials & scaffolds for tissue engineering, *Mater. Today*, 2011, **14**, 88–95.

2 S. Naahidi, M. Jafari, M. Logan, Y. J. Wang, Y. F. Yuan, H. Bae, B. Dixon and P. Chen, Biocompatibility of hydrogel-based scaffolds for tissue engineering applications, *Biotechnol. Adv.*, 2017, **35**, 530–544, DOI: 10.1016/j.biotechadv.2017.05.006.

3 D. M. Ibrahim, A. Kakarougkas and N. K. Allam, Recent advances on electrospun scaffolds as matrices for tissue-engineered heart valves, *Mater. Today Chem.*, 2017, **5**, 11–23, DOI: 10.1016/j.mtchem.2017.05.001.

4 K. A. Rieger, N. P. Birch and J. D. Schiffman, Designing electrospun nanofiber mats to promote wound healing—A review, *J. Mater. Chem. B*, 2013, **36**, 4531–4541.

5 J. D. Schiffman and C. L. Schauer, A review: electrospinning of biopolymer nanofibers and their applications, *Polym. Rev.*, 2008, **48**, 317–352.

6 R. M. A. Domingues, S. Chiera, P. Gershovich, A. Motta, R. L. Reis and M. E. Gomes, Enhancing the biomechanical performance of anisotropic nanofibrous scaffolds in tendon tissue engineering: reinforcement with cellulose nanocrystals, *Adv. Healthcare Mater.*, 2016, **5**, 1364–1375, DOI: 10.1002/adhm.201501048.

7 S. H. Lim and H. Q. Mao, Electrospun scaffolds for stem cells engineering, *Adv. Drug Delivery Rev.*, 2009, **61**, 1084–1096.

8 T. J. Sill and H. A. Von Recum, Electrospinning: applications in drug delivery and tissue engineering, *Biomaterials*, 2008, **29**, 1989–2006.

9 Q. P. Pham, U. Sharma and A. G. Mikos, Electrospinning of polymeric nanofibers for tissue engineering applications: a review, *Tissue Eng.*, 2006, **12**, 1197–1211, DOI: 10.1089/ten.2006.12.1197.

10 G. Yang, X. Li, Y. He, J. Ma, G. Ni and S. Zhou, From nano to micro to macro: electrospun hierarchically structured polymeric fibers for biomedical applications, *Prog. Polym. Sci.*, 2018, **81**, 80–113, DOI: 10.1016/j.progpolymsci.2017.12.003.

11 K. M. Nampoothiri, N. R. Nair and R. P. John, An overview of the recent developments in polylactide (PLA) research, *Bioresour. Technol.*, 2010, **101**, 8493–8501.

12 P. Simamora and W. Chern, Poly-L-lactic acid: an overview, *J. Drugs Dermatol.*, 2006, **5**, 436–440.

13 R. Auras, L.-T. Lim, S. E. M. Selke and H. Tsuji, *Poly(lactic acid) synthesis, structures, properties, processing, and applications*, John Wiley & Sons, New Jersey, 2010, DOI: 10.1002/9780470649848.

14 M. Vert, J. Mauduit and S. Li, Biodegradation of PLA/GA polymers: increasing complexity, *Biomaterials*, 1994, **15**, 1209–1213.

15 M. A. Elsawy, K.-H. Kim, J.-W. Park and A. Deep, Hydrolytic degradation of polylactic acid (PLA) and its composites, *Renewable Sustainable Energy Rev.*, 2017, **79**, 1346–1352, DOI: 10.1016/j.rser.2017.05.143.

16 P. B. Malafaya, G. A. Silva and R. L. Reis, Natural-based polymers as carriers and scaffolds for biomolecules and cell delivery in tissue engineering applications, *Adv. Drug Delivery Rev.*, 2007, **59**, 207–233.

17 L. Lisuzzo, G. Cavallaro, S. Milioto and G. Lazzara, Layered composite based on halloysite and natural polymers: a carrier for the pH controlled release of drugs, *New J. Chem.*, 2019, **43**, 10887.

18 N. Gull, S. M. Khan, M. T. Z. Butt, S. Khalid, M. Shafiq, A. Islam, S. Asim, S. Hafeez and R. U. Khan, In vitro study of chitosan-based multi-responsive hydrogels as drug release vehicles: a preclinical study, *RSC Adv.*, 2019, **9**, 31078.

19 V. A. Cataldo, G. Cavallaro, G. Lazzara, S. Milito and F. Parasi, Coffee grounds as filler for pectin: Green composites with competitive performances dependent on the UV irradiation, *Carbohydr. Polym.*, 2017, **170**, 198–205.

20 V. Beachley and X. Wen, Polymer nanofibrous structures: fabrication, biofunctionalization, and cell interaction, *Prog. Polym. Sci.*, 2010, **35**, 868–892, DOI: 10.1016/j.progpolymsci.2010.03.003.

21 C. Salas, Z. Thompson and N. Bhattarai, Electrospun chitosan fibers, in *Woodhead Publishing Series in Textiles, Electrospun Nanofibers*, ed. M. Afshari, Woodhead Publishing, 2017, pp. 371–398, DOI: 10.1016/B978-0-08-100907-9.00015-5.

22 R. Jayakumar, K. P. Chennazhi, R. A. A. Muzzarelli, H. Tamura, S. V. Nair and N. Selvamurugan, Chitosan conjugated DNA nanoparticles in gene therapy, *Carbohydr. Polym.*, 2010, **79**, 1–8.

23 M. Dash, F. Chillini, R. M. Ottenbrite and E. Chiellini, Chitosan – a versatile semi-synthetic polymer in biomedical applications, *Prog. Polym. Sci.*, 2011, **36**, 981–1014.

24 S. Huang and X. Fu, Naturally derived materials-based cell and drug delivery systems in skin regeneration, *J. Controlled Release*, 2010, **142**, 149–159, DOI: 10.1016/j.jconrel.2009.10.018.

25 S. Ahmed and S. Ikram, Chitosan based scaffolds and their applications in wound healing, *Achieve life sciences*, 2016, **10**, 27–37, DOI: 10.1016/j.als.2016.04.001.

26 M. Murariu and P. Dubois, PLA composites: from production to properties, *Adv. Drug Delivery Rev.*, 2016, **107**, 17–46, DOI: 10.1016/j.addr.2016.04.003.

27 Y. L. Cui, A. D. Qi, W. G. Liu, X. H. Wang, H. Wang, D. M. Ma and K. D. Yao, Biomimetic surface modification of poly(L-lactic acid) with chitosan and its effects on articular chondrocytes in vitro, *Biomaterials*, 2003, **24**, 3859–3868.

28 S. A. Martel-Estrada, C. A. Martínez-Pérez, J. G. Chacón-Nava, P. E. García-Casillas and I. Olivas-Armendariz, Synthesis and thermo-physical properties of chitosan/poly(DL-lactide-co-

glycolide) composites prepared by thermally induced phase separation, *Carbohydr. Polym.*, 2010, **81**, 775–783.

29 A. Elamparithi, A. M. Punnoose, S. F. D. Kuruvilla and S. Kuruvilla, Gelatin electrospun nanofibrous matrices for cardiac tissue engineering applications, *Int. J. Polym. Mater.*, 2017, **66**, 20–27.

30 Z. Chen, X. Mo and F. Qing, Electrospinning of collagen–chitosan complex, *Mater. Lett.*, 2007, **61**, 3490–3494.

31 F. Saporito, G. Sandri, M. C. Bonferoni, S. Rossi, L. Malavasi, C. Del Fante, B. Vigani, L. Black and F. Ferrari, Electrospun gelatin–chondroitin sulfate scaffolds loaded with platelet lysate promote immature cardiomyocyte proliferation, *Polymers*, 2018, **10**, 208, DOI: 10.3390/polym10020208.

32 K. Y. Lee, L. Jeong, Y. O. Kang, S. J. Lee and W. H. Park, Electrospinning of polysaccharides for regenerative medicine, *Adv. Drug Delivery Rev.*, 2009, **61**, 1020–1032.

33 R. Inai, M. Kotaki and S. Ramakrishna, Structure and property of electrospun PLLA single nanofibers, *Nanotechnology*, 2005, **16**, 208–213.

34 J. Xu, J. Zhang, W. Gao, H. Liang, H. Wang and J. Li, Preparation of chitosan/PLA blend micro/nanofibers by electrospinning, *Mater. Lett.*, 2009, **63**, 658–660, DOI: 10.1016/j.matlet.2008.12.014.

35 J. Andersen and J. Mack, Mechanochemistry and organic synthesis: from mystical to practical, *Green Chem.*, 2018, **20**, 1435–1443.

36 D. E. Crawford, C. K. G. Miskimmin, A. B. Albadarin, G. Walker and S. L. James, Organic synthesis by Twin Screw Extrusion (TSE): continuous, scalable and solvent-free, *Green Chem.*, 2017, **6**, 1507–1518, DOI: 10.1039/C6GC03413F.

37 S. Z. Rogovina, T. A. Akopova and G. A. Vikhoreva, Investigation of properties of chitosan obtained by solid-phase and suspension methods, *J. Appl. Polym. Sci.*, 1998, **70**, 927–933.

38 K. N. Bardakova, E. A. Grebenik, E. V. Istranova, L. P. Istranov, Y. V. Gerasimov, A. G. Grosheva, T. M. Zharikova, N. V. Minaev, B. S. Shavkuta, D. S. Dudova, S. V. Kostyuk, N. N. Vorob'eva, V. N. Bagratashvili, P. S. Timashev and R. K. Chailakhyan, Reinforced hybrid collagen sponges for tissue engineering, *Bull. Exp. Biol. Med.*, 2018, **165**, 142–147.

39 K. N. Bardakova, E. A. Grebenik, N. V. Minaev, S. N. Churbanov, Z. Moldagazyeva, G. E. Krupinov, S. V. Kostjuk and P. S. Timashev, *Mater. Sci. Eng., C*, 2020, **107**, 110300.

40 A. N. Ozerin, A. N. Zelenetskii, T. A. Akopova, S. N. Zelenetskii, L. V. Vladimirov, V. A. Zhorin, E. L. Mogilevskaya, A. O. Chernyshenko and G. A. Vikhoreva, Method of preparation of graft-copolymers of chitin and chitosan with synthetic polymers, RF Patent No. 2292354, 2007.

41 T. A. Akopova, A. N. Zelenetskii and A. N. Ozerin, Solid-state synthesis and modification of chitosan, in *Focus on Chitosan Research*, ed. A. N.Ferguson and A. G.O'Neill, Nova Science Publishers, New York, 2011, pp. 223–254.

42 T. S. Demina, K. N. Bardakova, N. V. Minaev, E. A. Svidchenko, A. V. Istomin, G. P. Goncharuk, L. V. Vladimirov, A. V. Grachev, A. N. Zelenetskii, P. S. Timashev and T. A. Akopova, Two-

photon-induced microstereolithography of chitosan-*g*-oligolactides as a function of their stereochemical composition, *Polymers*, 2017, **9**, 302, DOI: 10.3390/polym9070302.

43 T. A. Akopova, T. S. Demina, A. N. Shchegolikhin, T. S. Kurkin, C. Grandfils, N. S. Perov, A. S. Kechekyan and A. N. Zelenetskii, A novel approach to design chitosan-polyester materials for biomedical applications, *Int. J. Polym. Sci.*, 2012, **2012**, 827967, DOI: 10.1155/2012/827967.

44 T. S. Demina, C. Sevrin, C. Kapchiekue, T. A. Akopova and C. Grandfils, Chitosan-*g*-polyester microspheres: effect of length and composition of grafted chains, *Macromol. Mater. Eng.*, 2019, **304**, 1900203, DOI: 10.1002/mame.201900203.

45 V. M. Correlo, L. F. Boesel, M. Bhattacharya, J. F. Mano, N. M. Neves and R. L. Reis, Properties of melt processed chitosan and aliphatic polyester copolymers, *Mater. Sci. Eng., A*, 2005, **403**, 57–68.

46 L. Aliotta, P. Cinelli, M. B. Coltelli, M. C. Righetti, M. Gazzano and A. Lazzeri, Effect of nucleating agents on crystallinity and properties of poly(lactic acid) (PLA), *Eur. Polym. J.*, 2017, **93**, 822–832, DOI: 10.1016/j.eurpolymj.2017.04.041.

47 X. Zhu, S. Ni, T. Xia, Q. Yao, H. Li, B. Wang, J. Wang, X. Li and W. Su, Anti-neoplastic cytotoxicity of SN-38-loaded PCL/gelatin electrospun composite nanofiber scaffolds against human glioblastoma cells *in vitro*, *J. Pharm. Sci.*, 2015, **104**, 4345–4354, DOI: 10.1002/jps.24684.

48 E. N. Bolbasov, K. S. Stankevich, E. A. Sudarev, V. M. Bouznik, V. L. Kudryavtseva, L. V. Antonova, V. G. Matveeva, Y. G. Anissimov and S. I. Tverdokhlebov, The investigation of the production method influence on the structure and properties of the ferroelectric nonwoven materials based on vinylidene fluoride – tetrafluoroethylene copolymer, *Mater. Chem. Phys.*, 2016, **182**, 338–346.

49 A. B. Faia-Torres, M. Charnley, T. Goren, S. Guimond-Lischer, M. Rottmar, K. Maniura-Weber, N. D. Spencer, R. L. Reis, M. Textor and N. M. Neves, Osteogenic differentiation of human mesenchymal stem cells in the absence of osteogenic supplements: a surface-roughness gradient study, *Acta Biomater.*, 2015, **28**, 64–75.

50 M. Ortiz, R. Rosales-Ibáñez, A. Pozos-Guillén, C. de Bien, D. Toye, H. Flores and C. Grandfils, DPSC colonization of functionalized 3D textiles, *J. Biomed. Mater. Res., Part B*, 2017, **105**, 785–794, DOI: 10.1002/jbm.b.33609.

51 H. Tan, L. Zhao, S. Tian, H. Wen, X. Gou and T. Ngai, Gelatin particle-stabilized high-internal phase emulsions for use in oral delivery systems: protection effect and *in vitro* digestion study, *J. Agric. Food Chem.*, 2017, **65**, 900–907.

52 H. Tan, Z. Tu, H. Jia, X. Gou and T. Ngai, Hierarchical porous protein scaffold templated from high internal phase emulsion costabilized by gelatin and gelatin nanoparticles, *Langmuir*, 2018, **34**, 4820–4829, DOI: 10.1021/acs.langmuir.7b04047.

53 M. Xiao, A. Xu, T. Zhang and L. Hong, Tailoring the wettability of colloidal particles for pickering emulsions *via* surface modification and roughness, *Front. Chem.*, 2018, **6**, 225, DOI: 10.3389/fchem.2018.00225.